BRITISH JOURNAL OF HOSPITAL MEDICINE

ARTICLE

Prognostic Performance of the FLAMB Model in Primary Gastric Diffuse Large B-Cell Lymphoma

Jianbo Liu[1], Ao Li[1], Runhui Zheng[2], Haiying Wu[3], Yongqiang Wei[1], Ru Feng[1,*]

[1]Department of Hematology, Nanfang Hospital, Southern Medical University, Guangzhou, Guangdong, China
[2]Department of Hematology, The Fifth Affiliated Hospital of Guangzhou Medical University, Guangzhou, Guangdong, China
[3]Department of Radiation Oncology, Sun Yat-sen University Cancer Center, Guangzhou, Guangdong, China
*Correspondence: ruth1626@hotmail.com (Ru Feng)

Abstract

Aims/Background Primary gastric diffuse large B-cell lymphoma (PG-DLBCL) is a common gastrointestinal malignancy. While rituximab plus cyclophosphamide, doxorubicin, vincristine, and prednisone (R-CHOP)-based regimens have improved survival, reliable prognostic tools remain scarce. The International Prognostic Index (IPI), though validated for nodal DLBCL, shows limited accuracy in PG-DLBCL. To address this, we developed an intelligent prognostic model integrating key clinical variables to optimize individualized risk stratification, particularly for resource-limited clinical settings.

Methods A retrospective cohort study was conducted at Nanfang Hospital, Southern Medical University, enrolling patients diagnosed with PG-DLBCL between January 2007 and July 2022. Clinical data and survival outcomes were systematically collected. Optimal cut-off values were systematically determined for continuous variables using receiver operating characteristic (ROC) curve analysis. Survival rates were estimated using the Kaplan-Meier method, with survival curves plotted and univariate survival associations assessed using the log-rank test. Multivariable analyses were performed through Cox proportional hazards regression and random forest algorithms. A novel (ferritin, lactate dehydrogenase (LDH), age, monocyte count (mono), β2-microglobulin (β2-MG)) FLAMB prognostic model was constructed by integrating the Cox regression model with random forest classification. Model performance was evaluated by comparing its discriminative accuracy with that of the IPI scoring system.

Results Statistically significant differences in 5-year survival among PG-DLBCL patients were observed for ferritin, age, mono, LDH, β2-MG, B symptoms, and cell of origin (COO) in univariate survival analysis ($p < 0.05$). We developed the FLAMB model using five routinely available variables (ferritin, LDH, age, mono, and β2-MG) to enhance risk stratification in PG-DLBCL. Compared to the IPI, FLAMB demonstrated superior discriminative power (C-index: 0.653 vs. 0.637, $\Delta = 1.6\%$) and more effectively identified high-risk patients requiring treatment intensification. This enhanced risk stratification was confirmed by a statistically significant log-rank test ($p < 0.05$). Survival analysis in subgroups of non-germinal center B-cell like (GCB) and B symptoms-negative patients yielded consistent results.

Conclusion The newly developed FLAMB prognostic model offers more precise prognostic stratification than the IPI for patients with PG-DLBCL. FLAMB comprises five key variables derived from routine laboratory tests and general clinical characteristics, making it readily accessible. This model enables clinicians, particularly in primary care or community hospitals, to efficiently stratify patient risk, assess underlying disease severity, and inform timely treatment planning.

Key words: diffuse large B-cell lymphoma; stomach neoplasm; prognosis; risk assessment

Submitted: 13 March 2025 Revised: 6 April 2025 Accepted: 25 April 2025

How to cite this article:
Liu J, Li A, Zheng R, Wu H, Wei Y, Feng R. Prognostic Performance of the FLAMB Model in Primary Gastric Diffuse Large B-Cell Lymphoma. Br J Hosp Med. 2025. https://doi.org/10.12968/hmed.2025.0232

Introduction

Primary gastric diffuse large B-cell lymphoma (PG-DLBCL), the most common subtype of gastric non-Hodgkin lymphoma (NHL), exhibits distinct biological

behavior and clinical characteristics compared to nodal diffuse large B-cell lymphoma (DLBCL) (Bai and Zhou, 2021; Juárez-Salcedo et al, 2018). The current standard of care for PG-DLBCL involves combination therapy regimens centered on rituximab plus cyclophosphamide, doxorubicin, vincristine, and prednisone (R-CHOP), with or without local radiotherapy or surgery. However, significant heterogeneity persists in patient survival outcomes, with a subset of patients experiencing early relapse or refractory progression despite this multimodal approach (Avilés et al, 2004; Coiffier et al, 2002). Emerging evidence suggests that targeted therapies, including Bruton tyrosine kinase (BTK) inhibitors and cluster of differentiation 19 (CD19) chimeric antigen receptor T-cell (CAR-T) therapy, demonstrate promising efficacy in relapsed or refractory PG-DLBCL. However, major challenges remain in establishing standardized criteria for patient selection and identifying predictive biomarkers to guide treatment optimization (Trabolsi et al, 2024; Coughlin et al, 2025; Poletto et al, 2022).

Although numerous prognostic models exist for DLBCL, there remains a lack of relatively simple and rapid risk stratification tools for clinicians, especially for primary care or community hospital settings. The International Prognostic Index (IPI), while groundbreaking at the time of its development in 1993, demonstrates notable limitations in the contemporary immune-chemotherapy era (Ziepert et al, 2010). Temporal inadequacy is evident, as IPI — derived from pre-rituximab cohorts — systematically overestimates 5-year overall survival by 18.7% (95% confidence interval (CI): 15.2–22.3%) in R-CHOP-treated PG-DLBCL patients (George and Lakshmanan, 2024). Anatomic oversimplification further limits its utility, as IPI's "extra-nodal involvement" criterion overlooks gastric-specific pathobiology: 68% of PG-DLBCL cases demonstrate *Helicobacter pylori*-induced programmed death-ligand 1 (PD-L1) overexpression (Ruppert et al, 2020), while single-cell RNA sequencing data reveal distinct tumor microenvironment (TME) profiles in localized gastric lesions (Lugano I/II) compared to nodal DLBCL (Cui et al, 2025).

Methodologically, the IPI's reliance on Cox proportional hazards models (Ma et al, 2021) fails to capture non-linear biomarker interactions (e.g., ferritin-lactate dehydrogenase (LDH) synergy) and time-varying treatment effects, as evidenced by significant degradation in IPI performance in landmark survival analyses (p = 0.003). These combined limitations contribute to its suboptimal prognostic accuracy, with reported C-indices ranging from 0.59 to 0.63 across six independent PG-DLBCL validation cohorts (Wight et al, 2018).

Recent studies have confirmed that tumor microenvironmental factors are strongly associated with prognosis in PG-DLBCL. Elevated serum ferritin (Wan et al, 2024) and β2-microglobulin (β2-MG) levels (Chen et al, 2022) are independently associated with shorter overall survival (OS) and progression-free survival (PFS). However, current prognostic tools have not systematically integrated these markers. Circulating monocytes, via interleukin-6 (IL-6)/IL-10 paracrine signaling, contribute to Treg-dominated immunosuppressive niches (Bartoccioni et al, 2003), while elevated LDH remains a poor predictive indicator of survival outcome (Sehn et al, 2007). Beyond standard frailty metrics, age also influences host-TME interactions

by promoting immunosenescence-related CD8+ T-cell exhaustion, as evidenced by scRNA-seq cluster 15 (Cui et al, 2025).

Incorporating these TME-relevant factors, our study conducted univariate survival analysis in 137 PG-DLBCL patients and identified ferritin, LDH, age, monocyte count (mono), and β2-MG as significant predictors of 5-year overall survival. We subsequently developed a novel prognostic model (ferritin, LDH, age, mono, β2-MG) FLAMB, using Cox proportional hazards regression combined with random forest algorithms. This model integrates routinely accessible laboratory markers. The FLAMB model addresses key limitations of conventional prognostic tools by employing a hybrid machine learning approach (Cox regression + random forest) to capture complex biomarker interactions driven by the TME. It enables rapid, cost-effective risk stratification aligned with National Comprehensive Cancer Network (NCCN) guidelines, allowing community hospitals to promptly implement optimized, biologically-guided treatment approaches. This empowers clinicians to reduce diagnostic delays and translate precision oncology into actionable treatment workflows for managing gastric DLBCL.

Methods

Patient Selection Criteria

Patients were consecutively enrolled between January 2007 and July 2022 at Nanfang Hospital, Southern Medical University.

Inclusion Criteria

(1) Histopathological diagnosis: confirmed primary diffuse large B-cell lymphoma (DLBCL) based on International Classification of Diseases for Oncology (ICD-O)-3 morphological classification code 9680/3 (Shenoy et al, 2011), originating from the gastric corpus or antrum, as determined by gastroscopy or diagnostic biopsy. Immunohistochemical classification was performed using the Hans algorithm (Hans et al, 2004).

(2) Age $\geq$18 years at the time of diagnosis.

(3) First primary tumor, with no history of previous malignancies.

(4) Treatment-naïve patients scheduled to receive R-CHOP or CHOP-like regimens.

(5) Availability of complete baseline laboratory data (ferritin, LDH, β2-MG, and monocyte count, etc.) collected within 7 days pre-treatment.

Exclusion Criteria

(1) Coexistence with other lymphoma subtypes or transformed DLBCL.

(2) Evidence of central nervous system (CNS) or meningeal (parenchymal or meningeal) involvement.

(3) Major surgical procedures within 4 weeks before treatment initiation (excluding diagnostic procedures).

(4) Presence of severe heart, liver, lung, or kidney dysfunction.

(5) History of other tumors within the past 5 years.

(6) Incomplete data, including undocumented chemotherapy regimens or radiation therapy.

(7) Missing information about Ann Arbor stage or B symptoms status.

(8) The estimated life expectancy of less than 1 month.

Statistical Methods and Variable Selection

Statistical Methods and Software Applied

Continuous quantitative variables were analyzed using receiver operating characteristic (ROC) curve analysis to determine optimal cut-off values. ROC analysis was conducted using the scikit-learn package (version 1.6.1) in Python (version 3.11.1, Python Software Foundation, Beaverton, OR, USA), with visualizations generated accordingly. All continuous variables with biological relevance were subjected to ROC analysis. Variables with an area under the curve (AUC) >0.5 were retained for further analysis. Based on univariate survival analysis results, the log-rank test was used to verify associations between variables and survival time or outcome. A p-value < 0.05 was considered statistically significant.

Survival analyses were conducted for age, gender, Ann Arbor stage, IPI score, and comorbidity status, with significance assessed through log-rank test. Prognostic variables identified as statistically significant were further analyzed using Cox proportional hazards regression and a random forest model. These analyses were performed using the lifelines package (version 0.30.0) in Python (version 3.11.1). Risk stratification analysis of the prognostic models was evaluated through concordance index (C-index) calculations using the lifeline package. Additional statistical tests and analyses were performed using the scipy package (version 1.15.1).

Variable Selection and Model Construction

The variable selection and prognostic model construction process is shown in Fig. 1.

This flowchart illustrates the variable selection process for developing the final prognostic model in PG-DLBCL. Variables were categorized as continuous (analyzed using ROC curves to determine optimal cut-off values) or categorical (evaluated via log-rank tests). Predictors with statistical significance ($p < 0.05$ in Cox regression and variable of importance (VIMP) >0.1 in random forest analysis) were integrated into the final model.

A novel prognostic model was developed by integrating Cox proportional hazards regression with random forest significance analysis. Variables were included in the model if they met either of the following criteria: $p < 0.05$ in Cox regression or VIMP >0.1 in the random forest model. Consequently, variables were weighted based on their degree of contribution in the random forest and aligned with the principle of the IPI model. These selected variables were assigned scores and categorized into risk strata to facilitate clinical interpretation.

Model Validation

First, the C-index for the final and the IPI prognostic models was calculated. The final model score was used as a predictive risk score in this study, and its nega-

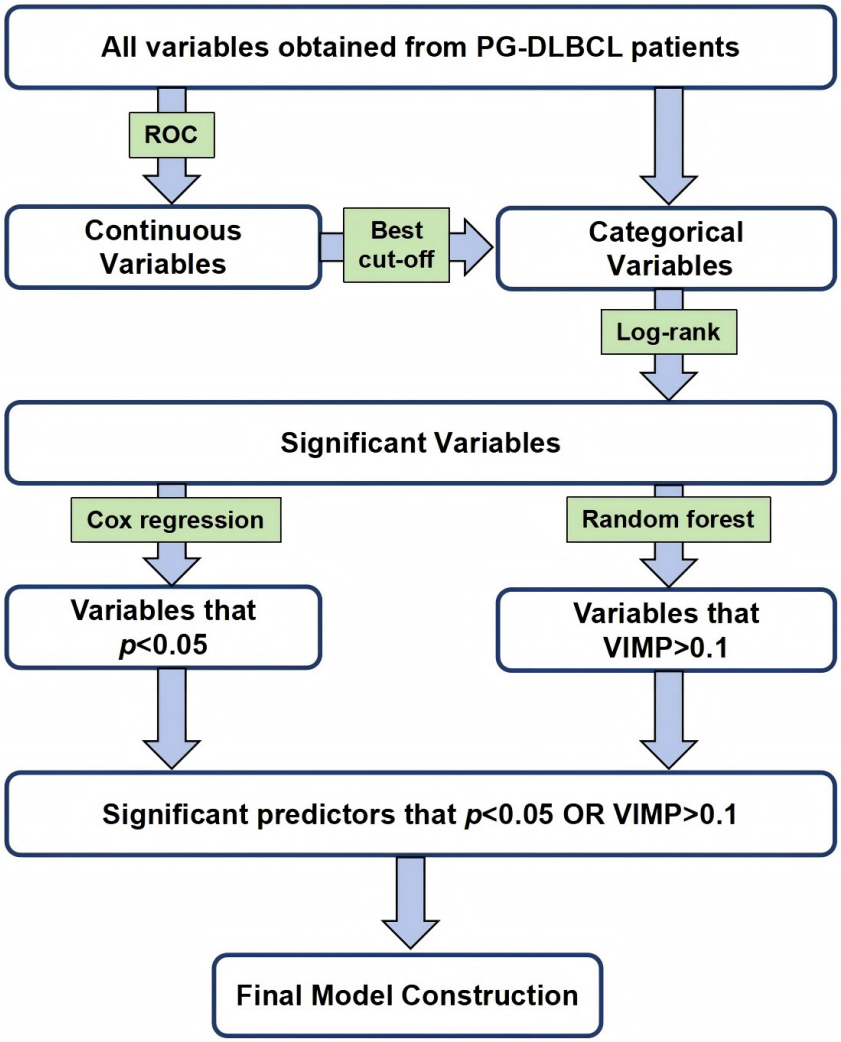

Fig. 1. Flowchart of variable selection and final model construction. PG-DLBCL, primary gastric diffuse large B-cell lymphoma; ROC, receiver operating characteristic; VIMP, variable of importance.

tive value was used to align with the underlying assumption of C-index calculation, namely, that higher predictive values correspond to shorter survival durations.

Finally, subgroup analyses were performed using the final prognostic model for all patients, stratified by cell of origin and B symptoms. Survival outcomes within each subgroup were then compared to those derived from the IPI model to evaluate the predictive performance in PG-DLBCL patients.

Results

Continuous Variable Analysis

Patient selection for PG-DLBCL was conducted at Nanfang Hospital, Southern Medical University (2007–2022). A total of 188 patients were initially screened, while 51 were excluded (secondary lymphoma: 16, incomplete data: 27, survival $<$1 month: 8), resulting in 137 patients included in the final analysis (Fig. 2). We systematically evaluated continuous variables for their prognostic significance us-

ing ROC curve analysis (**Supplementary Fig. 1**). As shown in Fig. 3, several biomarkers demonstrated notable discriminatory power for predicting 5-year overall survival (OS). Age was identified as a critical predictor, with a median value of 51.46 years (range: 18–79 years). Notably, elderly patients (≥61 years) accounted for 25.55% of the cohort, and the optimal age threshold for survival differentiation was identified as 61 years (95% CI: 26–79, $p = 0.043$; AUC = 0.54).

Monocyte count (mono) exhibited intermediate prognostic value, with an AUC of 0.62 and a cut-off value of 0.54×10^9/L (95% CI: 0.23–4.16, $p = 0.045$). Similarly, LDH demonstrated good discriminative ability (AUC = 0.63) with a threshold of 273 U/L (95% CI: 112.00–1161.00, $p = 0.013$). β2-MG showed strong predictive performance (AUC = 0.68) with a cut-off of 2.64 mg/L (95% CI: 1.45–8.17, $p = 0.001$). The median serum ferritin level was 183 ng/mL (95% CI: 9.70–1953.40, $p = 0.021$), ranging from a minimum of 5 ng/mL to a maximum of 1666 ng/mL. The ROC analysis yielded an AUC of 0.63, with an optimal cut-off value of 281 ng/mL.

Through ROC curve analysis, only indicators with an AUC >0.5 were retained for survival analysis. Based on these results, we selected the following cut-off values: age 61 years, mono 0.54×10^9/L, LDH 273 U/L, β2-MG 2.64 mg/L, and ferritin 281 ng/mL.

5-Year Survival Analysis

Using the selected cut-off values, we performed univariate survival analyses for all variables and compared their p-values (Table 1 and **Supplementary Fig. 2**).

The analysis identified seven variables with significant prognostic significance ($p < 0.05$), as visualized in Fig. 4. Kaplan-Meier survival analysis demonstrated statistically significant associations between key clinical variables and overall survival (log-rank $p < 0.05$ for all). These variables included age ($p = 0.036$), mono ($p = 0.001$), LDH ($p = 0.003$), β2-MG ($p = 0.006$), ferritin ($p = 0.022$), presence of B symptoms ($p = 0.027$), and cell of origin ($p = 0.007$). Survival curves stratified by these parameters revealed clear prognostic trends, where higher-risk subgroups (e.g., ≥61 years, elevated ferritin, mono, β2-MG or LDH, presence of B symptoms, and non-germinal center B-cell like origin) showed markedly reduced survival probabilities over time. These univariate findings collectively identified key variables for subsequent multivariable modeling, underscoring their potential to enhance risk stratification in PG-DLBCL.

Prognostic Model Construction

To identify the most relevant variables for survival prediction, we performed multivariable analyses incorporating those with significant univariate associations (Fig. 5). The integrated analysis highlighted mono, ferritin, and β2-microglobulin (β2-MG) as robust prognostic biomarkers across both Cox regression and random forest models. Monocyte count exhibited the highest statistical significance, followed by LDH ($p < 0.05$) (Fig. 5A). In the random forest importance ranking (Table 2 and Fig. 5B), β2-MG ranked highest (importance = 0.212), followed closely

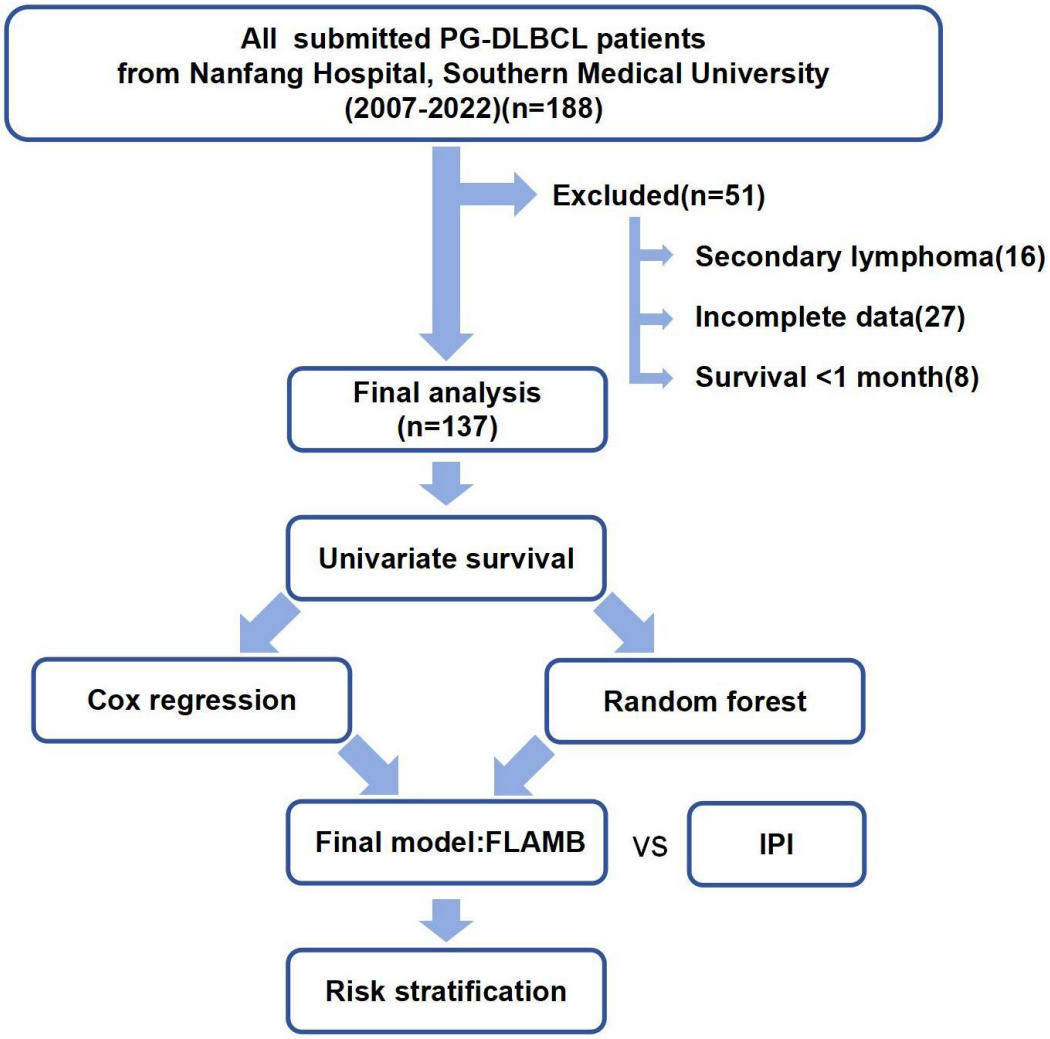

Fig. 2. Flowchart of PG-DLBCL patients Cohort. The figure showed patient selection for primary gastric diffuse large B-cell lymphoma (PG-DLBCL) at Nanfang Hospital, Southern Medical University (2007–2022). FLAMB, ferritin, lactate dehydrogenase (LDH), age, monocyte count (mono), β2-microglobulin (β2-MG); IPI, International Prognostic Index.

by ferritin (0.196) and LDH (0.180). Gini decrease (Fig. 5C) and accuracy decrease (Fig. 5D) further confirmed their predictive relevance.

We selected variables with $p < 0.05$ in the Cox multivariate regression analysis and importance scores >0.1 in the random forest model. Through iterative refinement using Cox proportional hazards regression and random forest algorithms, five core variables (ferritin, LDH, age, mono, β2-MG) were identified to construct the final prognostic model: the FLAMB model.

A risk stratification scheme was established based on variable scores in the FLAMB model (Table 3), categorized as follows: high-risk: 5 points; intermediate-risk: 2–4 points; low-risk: 0–1 points.

Prognostic Model Validation

The FLAMB model showed that the 5-year OS rate of the high-risk group (5 points) was significantly lower than that of the intermediate-risk group (2–4 points)

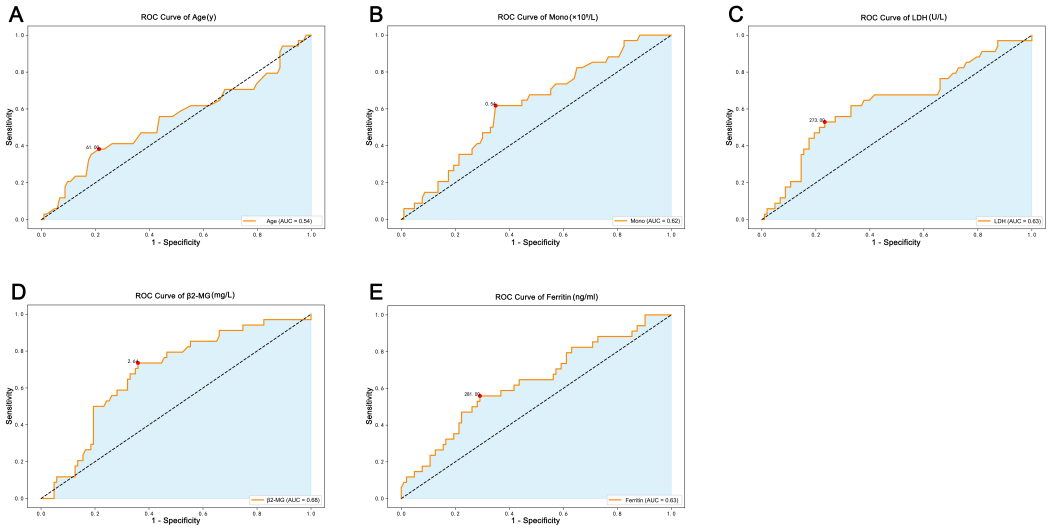

Fig. 3. ROC curves of variables selected for multivariate model construction (A–E). AUC, area under the curve.

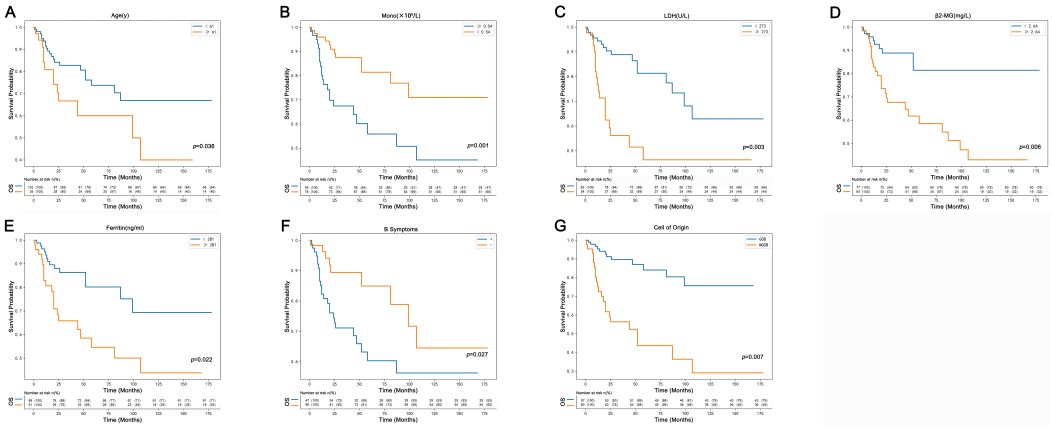

Fig. 4. Kaplan-Meier survival curves based on clinical variables (A–G). The curves illustrate Kaplan-Meier survival curves comparing overall survival across groups based on clinical variables: age, mono, LDH, β2-MG, ferritin, presence of B symptoms, and cell of origin. The y-axis represents survival probability, and the x-axis denotes time (months). Log-rank test p-values reflect statistically significant survival differences between groups ($p < 0.05$). OS, overall survival.

and the low-risk group (0–1 points) groups. The differences between these groups were statistically significant ($p = 0.0263$). In contrast, the IPI model could only distinguish the low-risk group from the low-intermediate-risk, high-intermediate-risk, and high-risk groups ($p = 0.0311$) (Fig. 6), with no statistically significant differences observed between certain adjacent groups, such as the high-intermediate-risk and the high-risk groups ($p = 0.15$; data not shown).

The FLAMB model demonstrated superior discriminatory performance in risk stratification (C-index = 0.653) compared to the IPI score (C-index = 0.637), and this improvement in stratification performance was statistically significant (log-rank $p < 0.05$).

To further validate the performance of our model, we examined two subgroups based on variables not integrated into the new model. In the B symptoms-stratified

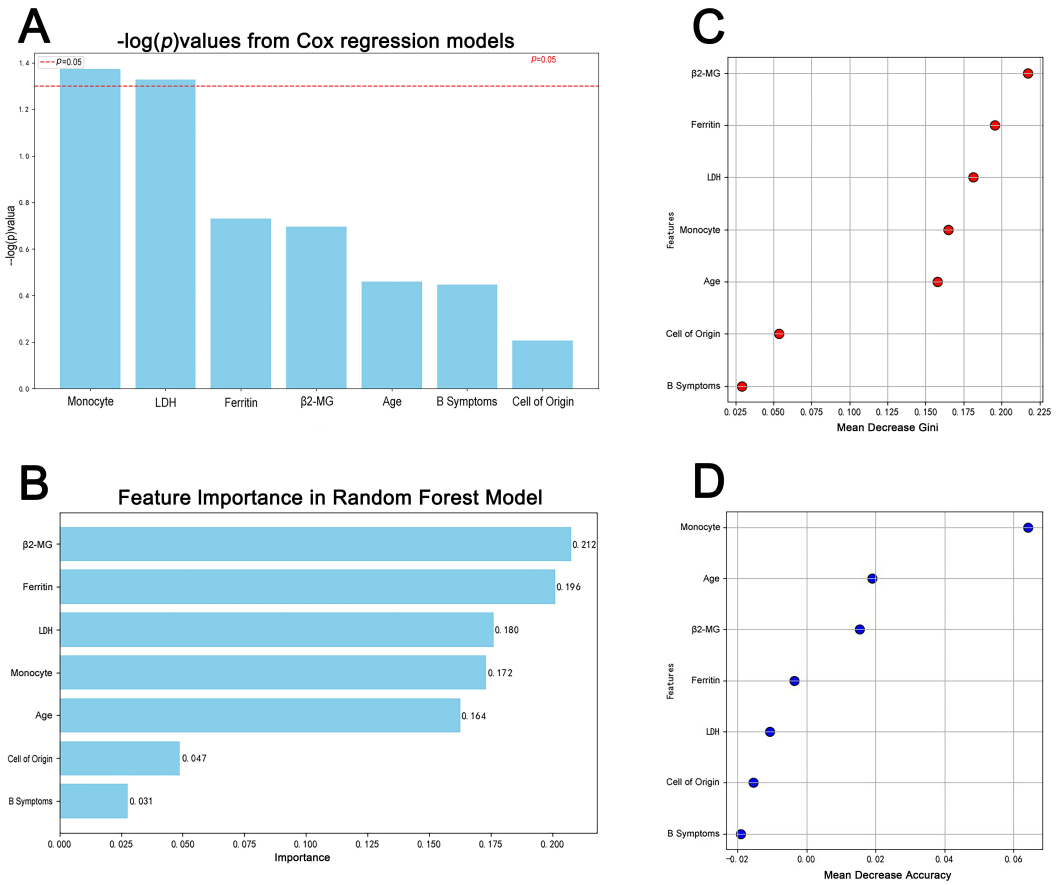

Fig. 5. Feature importance across predictive models. (A) Cox regression analysis showing –log (*p*) values for clinical variables, with monocyte count exhibiting the highest statistical significance. (B–D) Random forest-based feature importance metrics: (B) importance rankings, (C) decrease in Gini index, and (D) mean decrease in classification accuracy. Monocyte count, ferritin, and *β*2-MG consistently emerged as the top prognostic features.

analysis (Fig. 7A), the FLAMB model effectively distinguished survival outcomes across low-, intermediate-, and high-risk groups ($p = 0.021$). Similarly, in the cell-of-origin-stratified (Fig. 7B), the model maintained a significance ($p = 0.037$), with high-risk patients in the non-germinal center B-cell like (GCB) subgroup showing rapid survival decline, suggesting that the non-GCB phenotype may be associated with unique molecular vulnerabilities.

Subsequently, we applied the IPI prognostic model to validate these two subgroups. For the B symptoms-stratified cohort (Fig. 7C), survival trends were non-significant ($p = 0.096$), with overlapping curves in the intermediate-risk categories (low-intermediate-risk vs. high-intermediate-risk), indicating limited discriminatory power. In the cell-of-origin-stratified cohort (Fig. 7D), IPI fails to stratify non-GCB patients ($p = 0.126$), with overlapping survival curves between high-intermediate-risk and high-risk groups. Paradoxically, the high-intermediate-risk group transiently underperforms high-risk patients between 75–100 months.

Table 1. Baseline clinical characteristics of PG-DLBCL patients and 5-year survival outcomes.

Clinical feature	n (%)	Alive at 5 years, n (%)	*p*-value
Total	137	103 (75.18)	
Age (years)			**0.036**
≥61	35 (25.55)	24 (68.57)	
<61	102 (74.45)	79 (77.54)	
Gender			0.276
Male	78 (56.93)	58 (74.36)	
Female	59 (43.07)	45(76.27)	
Cell of origin			**0.007**
GCB	57 (41.61)	51 (89.47)	
Non-GCB	80 (58.39)	52 (65.00)	
LDH (U/L)			**0.003**
≥273	54 (39.42)	31 (57.41)	
<273	83 (60.58)	72 (86.75)	
BCL2 expression			0.341
Positive	96 (70.07)	71 (73.96)	
Negative	41 (29.93)	32 (78.05)	
BCL6 expression			0.297
Positive	113 (82.48)	84 (74.34)	
Negative	24 (17.52)	19 (79.17)	
B symptoms			**0.027**
Positive	47 (34.31)	32 (68.09)	
Negative	90 (65.69)	71 (78.89)	
Bone marrow involvement			0.753
Yes	13 (9.49)	10 (76.92)	
No	124 (90.51)	93 (75.00)	
Ann Arbor stage			0.059
1	27 (19.71)	24 (88.89)	
2	38 (27.74)	30 (78.95)	
3	15 (10.95)	8 (53.33)	
4	57 (41.61)	41 (71.93)	
IPI score			0.072
0	38 (27.74)	33 (86.84)	
1	29 (21.17)	25 (86.21)	
2	25 (18.25)	16 (64.00)	
3	29 (21.17)	19 (65.52)	
4	14 (10.22)	9 (64.29)	
5	2 (1.46)	1 (50.00)	
Monocyte count ($\times 10^9$/L)			**0.001**
≥0.54	59 (43.07)	37 (62.71)	
<0.54	78 (56.93)	66 (84.62)	
β2-MG (mg/L)			**0.006**
≥2.64	60 (43.80)	41 (68.33)	
<2.64	77 (56.20)	62 (80.52)	

Table 1. Continued.

Clinical feature	n (%)	Alive at 5 years, n (%)	*p*-value
Transplantation			0.593
Yes	7 (5.11)	5 (71.43)	
No	130 (94.89)	98 (75.38)	
Ferritin (ng/mL)			**0.022**
≥281	51 (37.23)	32 (62.75)	
<281	86 (62.77)	71 (82.56)	

p-values in bold indicate variables that are statistically significant in the tables.
GCB, germinal center B-cell like; BCL2, B-cell lymphoma-2.

Table 2. Variable importance in random forest model.

Variable	Importance score
*β*2-MG	0.212
Ferritin	0.196
LDH	0.180
Mono	0.172
Age	0.164
Cell of origin	0.047
B symptoms	0.031

Discussion

Diffuse large B-cell lymphoma (DLBCL) accounts for 30%–50% of all non-Hodgkin lymphoma (NHL) cases globally, with a disproportionately higher incidence observed in Asian populations (exceeding 40%). In China, approximately 36,000 new DLBCL cases are diagnosed annually, reflecting a growing public health concern. Notably, the incidence of primary gastric DLBCL demonstrates a strong positive correlation with the overall lymphoma burden, with a particularly marked upward trajectory in East Asian populations. PG-DLBCL represents the most common subtype of primary gastrointestinal lymphoma (PGIL), accounting for 60%–70% of cases (Alvarez-Lesmes et al, 2021; Zhu et al, 2023).

The standard first-line treatment for PG-DLBCL involves the R-CHOP regimen (rituximab + cyclophosphamide + doxorubicin + vincristine + prednisone), which has become the cornerstone of care (Stegemann et al, 2022; Hertzberg, 2022). Approximately 60% of early-stage patients are cured with the R-CHOP regimen (Ma'koseh et al, 2023; Vodicka et al, 2022), while 30%–40% experience primary resistance or relapse. For localized lesions, involved-field radiotherapy is commonly integrated following chemotherapy to enhance local control. Additionally, targeted therapies directed at specific molecular antigens, such as CD20 (rituximab) and BTK (ibrutinib) (Rho et al, 2023), along with CAR-T cell therapy (Duell and Westin, 2025; Wallace et al, 2025), have emerged as effective treatment options for relapsed or refractory cases, significantly improving remission rates.

Table 3. Variables cut-off values and assigned scores in the FLAMB model.

Variable	Cut-off value	FLAMB value
Ferritin	≥281 ng/mL	1
	<281 ng/mL	0
β2-MG	≥2.64 mg/L	1
	<2.64 mg/L	0
LDH	≥273 U/L	1
	<273 U/L	0
Age	≥61 years	1
	<61 years	0
Mono	$\geq 0.54 \times 10^9$/L	1
	$< 0.54 \times 10^9$/L	0

FLAMB model stratification: 5 points indicate high-risk, 2–4 points indicate intermediate-risk, and 0–1 points indicate low-risk.

The significant prognostic heterogeneity observed in gastric lymphoma underscores the critical need for precise risk stratification to optimize therapeutic outcomes. However, conventional models such as the International Prognostic Index (IPI) lack sufficient precision in stratifying patient risk, limiting their utility in personalized treatment planning. The IPI was originally developed using nodal DLBCL data, and core prognostic factors such as "extra-nodal involvement" may be overemphasized in PG-DLBCL. Emerging evidence suggests that tumor microenvironment-related factors (ferritin, β2-MG, etc.) are closely related to chemotherapy resistance and immunosuppressive microenvironment, which play key roles in the prognosis of DLBCL (Vaughan et al, 2024). One study has shown that high serum ferritin levels are significantly associated with reduced 5-year survival in PG-DLBCL patients (Zhang et al, 2015). Patients with β2-MG ≥3.5 mg/L have an increased risk of bone marrow involvement (Avilés et al, 2019). Additionally, a prospective study by Zöphel et al (2024) involving 46 newly diagnosed DLBCL patients reported that an elevated proportion of CD16+ monocytes was significantly associated with a higher risk of recurrence within 24 months ($p < 0.05$). These findings suggest the potential clinical value of these biomarkers of an immunosuppressive microenvironment. However, these indicators are not yet incorporated into the existing traditional assessment tools, highlighting the need to refine prognostic models to better reflect the biological complexity of PG-DLBCL.

In this study, ferritin, age, mono, LDH, and β2-MG were used to construct the FLAMB model, and its efficacy was compared with that of the IPI scoring model. The results showed that both prognostic models exhibited good discrimination ability and effectively stratified patients into different risk groups. Additionally, the overall comparison of the two models revealed statistically significant differences, underscoring the effectiveness of alternative risk-scoring systems

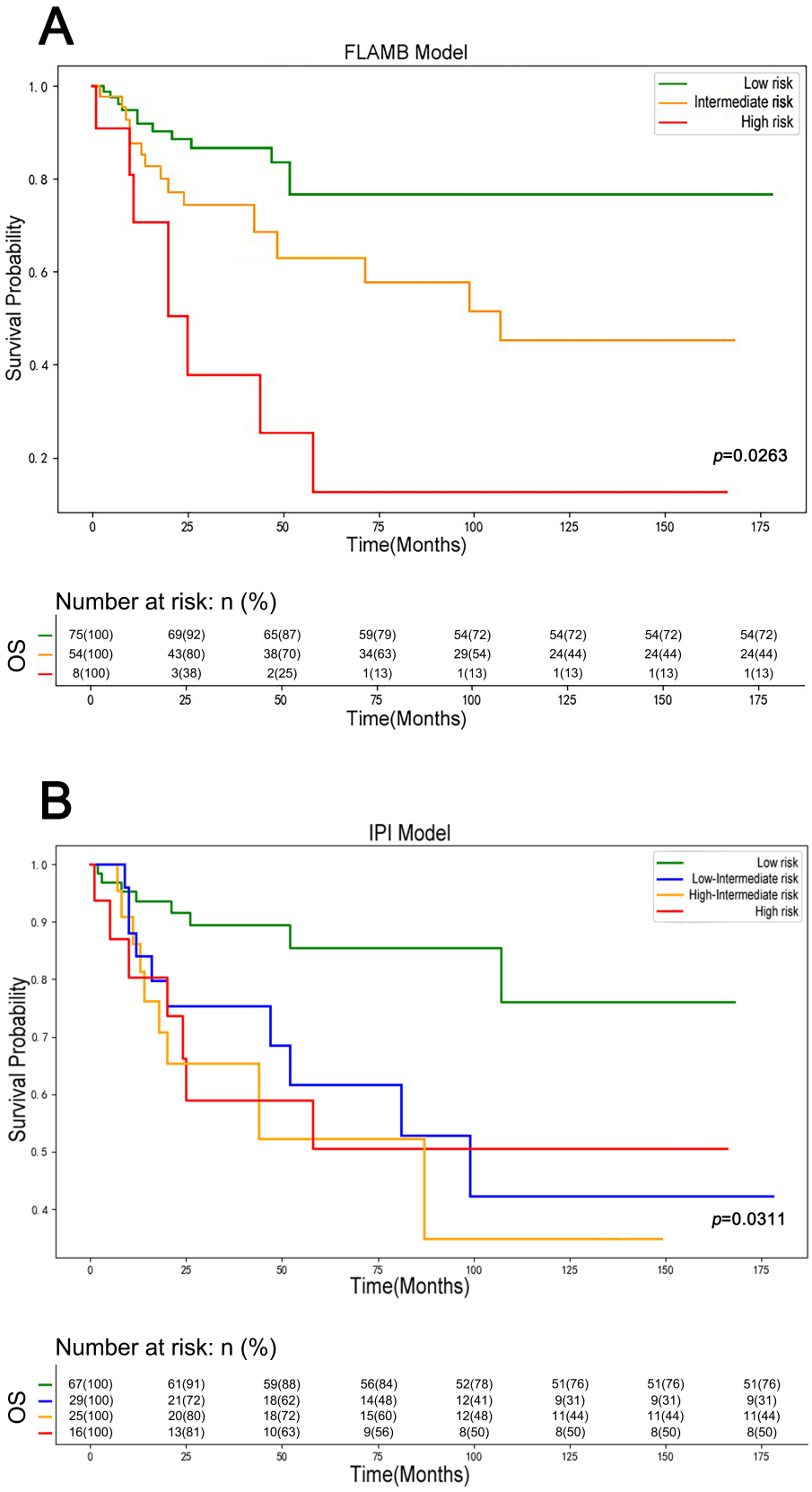

Fig. 6. Kaplan-Meier survival curves comparing risk stratification by FLAMB model (A) and IPI model (B).

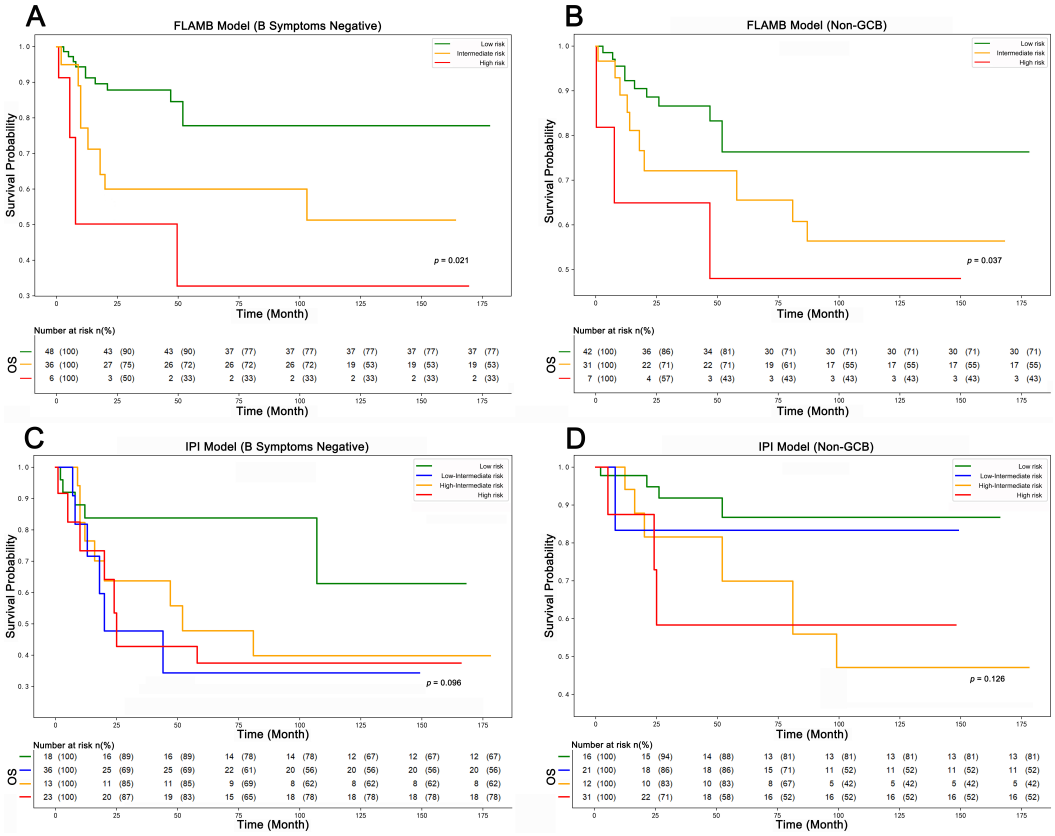

Fig. 7. Kaplan-Meier survival curves evaluating risk stratification by FLAMB (A,B) and IPI models (C,D) in clinical subgroups. (A,C) depict the B symptoms-negative subgroup, and (B,D) reflect the non-GCB subgroup. The FLAMB model shows statistically significant survival differences across risk groups (A: $p = 0.021$; B: $p = 0.037$), while the IPI model shows non-significant trends in B symptoms-stratified and cell-of-origin-stratified cohorts (C: $p = 0.096$; D: $p = 0.126$). The y-axis indicates survival probability, and the x-axis shows time (months).

in predicting patient survival outcomes. The FLAMB prognostic model significantly enhances risk stratification in PG-DLBCL and serves as a valuable complement to traditional prognostic models. Survival analysis within the non-GCB and B symptoms-negative subgroups yielded consistent results. FLAMB's superior performance likely stems from its integration of pathophysiologically relevant biomarkers (e.g., ferritin) rather than relying solely on clinical or demographic variables. Elevated ferritin, linked to inflammation and immune dysregulation, likely reflects microenvironmental stress, improving risk granularity.

The limited discriminatory capacity of IPI in non-GCB and B symptoms-negative cohorts (Fig. 7C,D) aligns with previous studies, which have questioned its relevance in biologically heterogeneous or inflammation-driven malignancies. Broad risk categories such as "high-intermediate-risk" may dilute critical prognostic signals. Importantly, FLAMB biomarkers (LDH, β2-MG, ferritin) are measurable via routine blood tests, reducing dependence on costly imaging modalities such as positron emission tomography-computed tomography (PET-CT) required by the IPI model. In resource-constrained settings, FLAMB could facilitate the early iden-

tification and triage of high-risk patients (5-year OS: 41%) to tertiary centers for intensive therapeutic intervention, potentially reducing treatment delays.

FLAMB model-driven risk stratification informs tailored treatment intensification. Patients classified as high-risk by FLAMB (score $\geq$3) may benefit from biomarker-driven therapeutic interventions. An elevated monocyte count ($\geq$0.54 $\times$ 10^9/L) is associated with an immunosuppressive TME, suggesting potential synergy between programmed death receptor-1 (PD-1) inhibitors (e.g., pembrolizumab) and R-CHOP. Additionally, ferritin-high patients ($\geq$281 ng/mL) may respond to iron chelation therapy (e.g., deferasirox), which reverses chemotherapy resistance and improves overall response rates (ORR: +27%) in preclinical models.

However, this study has several limitations. First, the single-center, retrospective design with a modest sample size limits statistical power and increases the risk of overfitting, particularly given the model's inclusion of multiple covariates (e.g., 7 variables). Larger, prospectively enrolled cohorts are required to confirm the robustness of the FLAMB model. Second, although FLAMB demonstrated superior discriminative power compared to the IPI model, it faces critical validation gaps. The lack of internal validation (e.g., bootstrapping) and external validation in multi-center cohorts (e.g., international lymphoma consortia), along with the lack of cross-validation, raises concerns about potential overfitting and limited generalizability. The retrospective, single-center design (Nanfang Hospital, Southern Medical University introduces selection bias, especially given the ethnically homogeneous population (100% Chinese) and the exclusion of gastric-specific confounding factors (e.g., *Helicobacter pylori* infection status, present in 68% of gastric DLBCL cases). Third, FLAMB's variables (e.g., monocyte count, ferritin) were selected based on statistical associations rather than mechanistic insights. This limits the model's translational potential to guide targeted therapies (e.g., PD-1 inhibitors for monocyte-high subsets). Moreover, dynamic monitoring remains insufficient. The model relies solely on baseline diagnostic data and does not account for changes in key indicators during the treatment process (such as post-treatment complications or achievement of molecular remission). Lastly, the study did not integrate molecular features, including genomic subtypes (e.g., double- or triple-hit lymphoma) or genetic alterations (e.g., myelocytomatosis oncogene/B-cell lymphoma-2 (MYC/BCL2) rearrangements) into the final model.

To address these limitations, rigorous validation frameworks should prioritize three key areas. First, multi-center studies should evaluate FLAMB across ethnically diverse populations and treatment eras to confirm generalizability. Second, dynamic risk modeling should be employed to enhance prognostic accuracy by generating longitudinal FLAMB scores updated at critical clinical milestones to capture evolving biomarkers such as β2-MG trends or ferritin fluctuations during therapy. Additionally, time-split cross-validation should be implemented to assess FLAMB's robustness in modern immunotherapy contexts, where novel agents may alter risk trajectories. Collectively, these strategies would transform FLAMB from a static predictor into an adaptive, context-aware tool for precision oncology.

Conclusion

The FLAMB model developed in this study significantly improves risk stratification in patients with PG-DLBCL. This model not only validates the independent predictive value of traditional prognostic indicators but also incorporates ferritin and mono subsets into the prognostic system for the first time, addressing the limitations of the conventional IPI score, which does not account for features of the immune microenvironment.

Key Points

- The FLAMB model (ferritin, LDH, age, mono, β2-MG) enhances risk prediction in gastric DLBCL, outperforming the International Prognostic Index.
- FLAMB stratifies patients into low-, intermediate-, and high-risk groups, improving 5-year survival prediction, particularly for early relapse identification.
- FLAMB utilizes routine laboratory markers (e.g., ferritin, β2-MG), enabling cost-effective risk assessment in resource-limited settings, especially in primary and community hospitals, to support timely treatment adjustments.
- The retrospective design and single-center cohort require external validation and integration with emerging biomarkers (e.g., PD-L1).

Availability of Data and Materials

The data used to support the findings of this study are available from the corresponding author upon request.

Author Contributions

RF, YQW designed the research study. JBL and AL performed the research and analyzed the data. RHZ made substantial contributions to the acquisition and analysis of clinical data. HYW contributed significantly to data analysis and statistical support, ensuring the robustness of the findings. JBL wrote the first draft. All authors contributed to revising the manuscript critically for important intellectual content. All authors read and approved the final manuscript. All authors have participated sufficiently in the work and agreed to be accountable for all aspects of the work.

Ethics Approval and Consent to Participate

The study was conducted in accordance with the Declaration of Helsinki (as revised in 2013). The current study protocol was approved by the Ethics Committee of Nanfang Hospital, Southern Medical University (No. NEFC2020-R090). All

patients gave written informed consent themselves prior to treatment, allowing the use of their medical records for medical research.

Acknowledgement

Not applicable.

Funding

This research received no external funding.

Conflict of Interest

The authors declare no conflict of interest.

Supplementary Material

Supplementary material associated with this article can be found, in the online version, at https://www.magonlinelibrary.com/doi/suppl/10.12968/hmed.2025.0232.

References

Alvarez-Lesmes J, Chapman JR, Cassidy D, Zhou Y, Garcia-Buitrago M, Montgomery EA, et al. Gastrointestinal Tract Lymphomas. Archives of Pathology & Laboratory Medicine. 2021; 145: 1585–1596. https://doi.org/10.5858/arpa.2020-0661-RA

Avilés A, Nambo MJ, Neri N, Huerta-Guzmán J, Cuadra I, Alvarado I, et al. The role of surgery in primary gastric lymphoma: results of a controlled clinical trial. Annals of Surgery. 2004; 240: 44–50. https://doi.org/10.1097/01.sla.0000129354.31318.f1

Avilés A, Nambo MJ, Neri N. Primary gastric diffuse large B-cell lymphoma: The role of dose-dense chemotherapy. Journal of Oncology Pharmacy Practice. 2019; 25: 1682–1686. https://doi.org/10.1177/1078155218809458

Bai Z, Zhou Y. A systematic review of primary gastric diffuse large B-cell lymphoma: Clinical diagnosis, staging, treatment and prognostic factors. Leukemia Research. 2021; 111: 106716. https://doi.org/10.1016/j.leukres.2021.106716

Bartoccioni E, Scuderi F, Marino M, Provenzano C, Kaplanski G, Marin V, et al. IL-6, monocyte infiltration and parenchymal cells. Trends in Immunology. 2003; 24: 298–299. https://doi.org/10.1016/s1471-4906(03)00112-1

Chen H, Zhong Q, Zhou Y, Qin Y, Yang J, Liu P, et al. Enhancement of the International prognostic index with β2-microglobulin, platelet count and red blood cell distribution width: a new prognostic model for diffuse large B-cell lymphoma in the rituximab era. BMC Cancer. 2022; 22: 583. https://doi.org/10.1186/s12885-022-09693-z

Coiffier B, Lepage E, Briere J, Herbrecht R, Tilly H, Bouabdallah R, et al. CHOP chemotherapy plus rituximab compared with CHOP alone in elderly patients with diffuse large-B-cell lymphoma. The New England Journal of Medicine. 2002; 346: 235–242. https://doi.org/10.1056/NEJMoa011795

Coughlin CA, Chahar D, Lekakis M, Youssfi AA, Li L, Roberts E, et al. Bruton's tyrosine kinase inhibition re-sensitizes multidrug-resistant DLBCL tumors driven by BCL10 gain-of-function mutants to venetoclax. Blood Cancer Journal. 2025; 15: 9. https://doi.org/10.1038/s41408-025-01214-y

Cui Y, Hu G, Han X, Li W, Wang X, Qian Z, et al. Comprehensive Analysis of Single-Cell and Bulk Transcriptomics Identified Regulatory T-Cell Features as Predictors of Prognosis in Diffuse Large B-Cell Lymphoma. Hematological Oncology. 2025; 43: e70050. https://doi.org/10.1002/hon.70050

Duell J, Westin J. The future of immunotherapy for diffuse large B-cell lymphoma. International Journal of Cancer. 2025; 156: 251–261. https://doi.org/10.1002/ijc.35156

George DM, Lakshmanan A. Lymphomas With Primary Gastrointestinal Presentation: A Retrospective Study Covering a Five-Year Period at a Quaternary Care Center in Southern India. Cureus. 2024; 16: e75161. https://doi.org/10.7759/cureus.75161

Hans CP, Weisenburger DD, Greiner TC, Gascoyne RD, Delabie J, Ott G, et al. Confirmation of the molecular classification of diffuse large B-cell lymphoma by immunohistochemistry using a tissue microarray. Blood. 2004; 103: 275–282. https://doi.org/10.1182/blood-2003-05-1545

Hertzberg M. R-CHOP in DLBCL: priming for success. Blood. 2022; 139: 1121–1122. https://doi.org/10.1182/blood.2021013620

Juárez-Salcedo LM, Sokol L, Chavez JC, Dalia S. Primary Gastric Lymphoma, Epidemiology, Clinical Diagnosis, and Treatment. Cancer Control. 2018; 25: 1073274818778256. https://doi.org/10.1177/1073274818778256

Ma SY, Tian XP, Cai J, Su N, Fang Y, Zhang YC, et al. A prognostic immune risk score for diffuse large B-cell lymphoma. British Journal of Haematology. 2021; 194: 111–119. https://doi.org/10.1111/bjh.17478

Ma'koseh M, Farfoura H, Abufara A, Elmusa R, Hushki A, Faqeer N, et al. Outcome and patterns of relapse in primary gastric diffuse large B cell lymphoma treated with RCHOP. Hematology. 2023; 28: 2198898. https://doi.org/10.1080/16078454.2023.2198898

Poletto S, Novo M, Paruzzo L, Frascione PMM, Vitolo U. Treatment strategies for patients with diffuse large B-cell lymphoma. Cancer Treatment Reviews. 2022; 110: 102443. https://doi.org/10.1016/j.ctrv.2022.102443

Rho H, Jeong IJH, Prica A. Ibrutinib Plus RCHOP versus RCHOP Only in Young Patients with Activated B-Cell-like Diffuse Large B-Cell Lymphoma (ABC-DLBCL): A Cost-Effectiveness Analysis. Current Oncology. 2023; 30: 10488–10500. https://doi.org/10.3390/curroncol30120764

Ruppert AS, Dixon JG, Salles G, Wall A, Cunningham D, Poeschel V, et al. International prognostic indices in diffuse large B-cell lymphoma: a comparison of IPI, R-IPI, and NCCN-IPI. Blood. 2020; 135: 2041–2048. https://doi.org/10.1182/blood.2019002729

Sehn LH, Berry B, Chhanabhai M, Fitzgerald C, Gill K, Hoskins P, et al. The revised International Prognostic Index (R-IPI) is a better predictor of outcome than the standard IPI for patients with diffuse large B-cell lymphoma treated with R-CHOP. Blood. 2007; 109: 1857–1861. https://doi.org/10.1182/blood-2006-08-038257

Shenoy PJ, Malik N, Nooka A, Sinha R, Ward KC, Brawley OW, et al. Racial differences in the presentation and outcomes of diffuse large B-cell lymphoma in the United States. Cancer. 2011; 117: 2530–2540. https://doi.org/10.1002/cncr.25765

Stegemann M, Denker S, Schmitt CA. DLBCL 1L—what to expect beyond R-CHOP? Cancers. 2022; 14: 1453. https://doi.org/10.3390/cancers14061453

Trabolsi A, Arumov A, Schatz JH. Bispecific antibodies and CAR-T cells: dueling immunotherapies for large B-cell lymphomas. Blood Cancer Journal. 2024; 14: 27. https://doi.org/10.1038/s41408-024-00997-w

Vaughan J, Wiggill T, Mia Z, Patel M. Tumour-associated macrophages in diffuse large B-cell lymphoma: the prognostic and therapeutic impact in a South African centre with high HIV seroprevalence. Immunologic Research. 2024; 72: 1393–1403. https://doi.org/10.1007/s12026-024-09537-x

Vodicka P, Klener P, Trneny M. Diffuse Large B-Cell Lymphoma (DLBCL): Early Patient Management and Emerging Treatment Options. OncoTargets and Therapy. 2022; 15: 1481–1501. https://doi.org/10.2147/OTT.S326632

Wallace DS, Loh KP, Casulo C. How I treat older patients with relapsed/refractory diffuse large B-cell lymphoma. Blood. 2025; 145: 277–289. https://doi.org/10.1182/blood.2024024788

Wan M, Zhang W, Huang H, Fang X, Chen Y, Tian Y, et al. Development and validation of a novel prognostic nomogram for advanced diffuse large B cell lymphoma. Clinical and Experimental Medicine. 2024; 24: 64. https://doi.org/10.1007/s10238-024-01326-y

Wight JC, Chong G, Grigg AP, Hawkes EA. Prognostication of diffuse large B-cell lymphoma in the molecular era: moving beyond the IPI. Blood Reviews. 2018; 32: 400–415. https://doi.org/10.1016/j.blre.2018.03.005

Zhang S, Wang L, Yu D, Shen Y, Cheng S, Zhang L, et al. Localized primary gastrointestinal diffuse large B cell lymphoma received a surgical approach: an analysis of prognostic factors and comparison of staging systems in 101 patients from a single institution. World Journal of Surgical Oncology. 2015; 13: 246. https://doi.org/10.1186/s12957-015-0668-5

Zhu T, Lei H, Wang YH, Liu LP, Lei YL, Wang N, et al. Primary gastrointestinal lymphoma with intestinal perforation. QJM: Monthly Journal of the Association of Physicians. 2023; 116: 125–126. https://doi.org/10.1093/qjmed/hcac227

Ziepert M, Hasenclever D, Kuhnt E, Glass B, Schmitz N, Pfreundschuh M, et al. Standard International prognostic index remains a valid predictor of outcome for patients with aggressive CD20+ B-cell lymphoma in the rituximab era. Journal of Clinical Oncology. 2010; 28: 2373–2380. https://doi.org/10.1200/JCO.2009.26.2493

Zöphel S, Küchler N, Jansky J, Hoxha C, Schäfer G, Weise JJ, et al. CD16+ as predictive marker for early relapse in aggressive B-NHL/DLBCL patients. Molecular Cancer. 2024; 23: 210. https://doi.org/10.1186/s12943-024-02123-7